Pyramidal Inversion at Phosphorus Facilitated by the Presence of Proximate Lewis Acids. Coordination Chemistry of Group 13 Elements with the Macrocyclic Bis(amidophosphine) Ligand [P_2N_2] ([P_2N_2] = [PhP($CH_2SiMe_2NSiMe_2CH_2$)$_2$PPh])

Michael D. Fryzuk,* Garth R. Giesbrecht, and Steven J. Rettig[†]

Department of Chemistry, University of British Columbia, 2036 Main Mall, Vancouver, B.C., Canada V6T 1Z1

Received May 28, 1998

Investigations on the preparation of four- and five-coordinate aluminum and gallium bis(amidophosphine) derivatives are reported. The reaction of the macrocyclic ligand precursor *anti*-$Li_2(THF)_2[P_2N_2]$ ([P_2N_2] = [PhP(CH_2SiMe_2-$NSiMe_2CH_2$)$_2$PPh]) with $AlCl_3$ or $GaCl_3$ in toluene at 25 °C leads to the formation of the four-coordinate species *anti*-MCl[P_2N_2] (M = Al (**1**), Ga (**2**)). An X-ray diffraction study of *anti*-GaCl[P_2N_2] shows it to be monomeric with a distorted tetrahedral geometry at Ga; only one of the phosphine donors of the [P_2N_2] ligand binds to the gallium, resulting in the retention of the *anti*-configuration. The solution NMR spectra are consistent with C_s symmetry. The addition of $AlCl_3$ or $GaCl_3$ to the macrocyclic ligand precursor *syn*-Li_2(dioxane)[P_2N_2] in toluene at 25 °C yields the five-coordinate complexes *syn*-MCl[P_2N_2] (M = Al (**3**), Ga (**4**)). The X-ray crystal structure of *syn*-GaCl[P_2N_2] reveals a trigonal bipyramidal geometry about the metal atom, necessitating the coordination of both phosphorus atoms. The solution NMR spectra are consistent with a C_{2v} symmetric complex. Heating the anti complexes results in the clean conversion to the syn complexes, with pyramidal inversion observed at phosphorus. The kinetics of this inversion were studied by ^{1}H NMR spectroscopy and found to be first-order. Barriers to pyramidal inversion ($\Delta G^{\ddagger}$) were calculated to be 29.1 and 30.1 kcal mol^{-1} for the aluminum and gallium complexes, respectively; these barriers are approximately 2−3 kcal mol^{-1} lower than that determined for the metal-free, protonated compounds *anti*- and *syn*-$H_2[P_2N_2]$. It is suggested that the role that the metals play in this inversion, based on the values of $\Delta G^{\ddagger}$, involves the large negative entropies of activation and thus help organize the transition state.

Introduction

One of the most fundamental stereoisomerization processes is pyramidal inversion.[1] For amines, inversion is extremely facile with activation barriers that range from 5 to 10 kcal/mol.[2−5] However, for tertiary phosphines the barriers are considerably higher, ranging from 30 to 38 kcal/mol,[1,6−9] and this has allowed for the separation and study of enantiomeric and diastereomeric forms of simple monodentate and bidentate chiral phosphine systems.[10] In fact, typical minimum conditions for inversion of a pyramidal tertiary phosphine require heating at 150 °C for 15 h.[11] A number of factors have been identified as affecting the barrier to inversion at phosphorus, and these include steric effects, the presence of conjugation (or hyperconjugation), effects of angular constriction, and the presence of heteroatom substituents. In this work, we examine the effect of a distal Lewis acidic metal center on the inversion barrier of a remote pyramidal phosphine donor in a macrocyclic ring that contains two phosphine and two amido donors. Whereas macrocycles with sp^3 amine donors do not exhibit stereoisomers due to rapid pyramidal inversion, macrocycles that contain sp^3 phosphines generally form as mixtures of stereoisomers, a direct result of high barriers to pyramidal inversion.[12]

Coordination of a phosphine ligand to a metal center is expected to occur with retention of configuration at phosphorus and because the coordinated phosphine becomes tetrahedral, the inversion process is necessarily arrested. In this paper, we report our findings on the coordination chemistry of the macrocyclic ligand [P_2N_2] (where [P_2N_2] = [PhP($CH_2SiMe_2NSiMe_2CH_2$)$_2$-PPh]) with the Lewis acidic group 13 elements, Al and Ga. The macrocycle can be isolated in two pseudo-stereoisomeric forms which differ mainly as a result of the relative stereochemistry at the two phosphorus donors (syn and anti forms). These two forms show different coordination chemistry with both aluminum and gallium which allowed us to study the inversion process and show how the presence of Lewis acidic centers in close proximity to an uncoordinated phosphine ligand can result in an entropically governed increase in the rate of pyramidal inversion.

[†] Experimental Officer: UBC Structural Chemistry Laboratory. Deceased, October 27, 1998.

(1) Rauk, A.; Allen, L. C.; Mislow, K. *Angew. Chem., Int. Ed. Engl.* **1970**, *9*, 400.
(2) Anet, F. A. L.; Trepka, R. D.; Cram, D. J. *J. Am. Chem. Soc.* **1967**, *89*, 357.
(3) Swalen, J. D.; Ibers, J. A. *J. Chem. Phys.* **1962**, *36*, 1914.
(4) Lambert, J. B.; Oliver, W. L., Jr. *J. Am. Chem. Soc.* **1969**, *91*, 7774.
(5) Gribble, G. W.; Easton, J.; Eaton, J. T. *Tetrahedron Lett.* **1970**, *13*, 1075.
(6) Lehn, J. M.; Munsch, B. *J. Chem. Soc., Chem. Commun.* **1969**, 1327.
(7) Baechler, R. D.; Farnham, W. B.; Mislow, K. *J. Am. Chem. Soc.* **1969**, *91*, 5686.
(8) Baechler, R. D.; Mislow, K. *J. Am. Chem. Soc.* **1970**, *92*, 3090.
(9) Baechler, R. D.; Mislow, K. *J. Am. Chem. Soc.* **1971**, *93*, 773.
(10) Imamoto, T.; Watanabe, J.; Wada, Y.; Masuda, H.; Yamada, H.; Tsuruta, H.; Matsukawa, S.; K., Y. *J. Am. Chem. Soc.* **1998**, *120*, 1635.
(11) Edwards, P. G.; Fleming, J. S.; Liyanage, S. S. *Inorg. Chem.* **1996**, *35*, 4563.
(12) Caminade, A. M.; Majoral, J. P. *Chem. Rev.* **1994**, *94*, 1183.

10.1021/ic9805978 CCC: $15.00
Published on Web 12/05/1998

Experimental Section

Procedures. Unless otherwise stated all manipulations were performed under an atmosphere of dry, oxygen-free nitrogen or argon by means of standard Schlenk or glovebox techniques. The glovebox used was a Vacuum Atmospheres HE-553-2 model equipped with a MO-40-2H purification system and a −40 °C freezer. ^{1}H and ^{31}P{^{1}H} NMR spectroscopy were performed on an AMX 500 instrument operating at 500.1 and 121.4 MHz, respectively. ^{1}H NMR spectra were referenced to internal C_6D_5H (7.15 ppm) or $C_6D_5CD_2H$ (2.09 ppm). ^{31}P{^{1}H} NMR spectra were referenced to external $P(OMe)_3$ (141.0 ppm with respect to 85% H_3PO_4 at 0.0 ppm). Mass spectral studies were carried out on a Kratos MS 50 using an EI source. Microanalyses (C, H, N) were performed by Mr. P. Borda of this department.

Materials. *anti*-$Li_2(THF)_2[P_2N_2]$ and *syn*-Li_2(dioxane)$[P_2N_2]$ were prepared by published procedures.[13] *anti*-$H_2[P_2N_2]$ and *syn*-$H_2[P_2N_2]$ were synthesized by the addition of solid $Me_3NH^+Cl^-$ (2 equiv) to toluene solutions of the lithium salts,[14] followed by filtration. $AlCl_3$ and $GaCl_3$ were purchased from Strem and used as received. Toluene was refluxed over CaH_2 prior to a final distillation from sodium benzophenone ketyl under an argon atmosphere. Deuterated solvents were dried by distillation from sodium benzophenone ketyl; oxygen was removed by 3 freeze−pump−thaw cycles.

***anti*-AlCl[P$_2$N$_2$] (1).** To a slurry of $AlCl_3$ (60 mg; 0.450 mmol) in toluene (5 mL) was added a toluene solution (10 mL) of *anti*-$Li_2(THF)_2[P_2N_2]$, (300 mg; 0.43 mmol). The reaction mixture was stirred for 12 h and then passed through a frit lined with Celite to remove LiCl. The solvent was removed in vacuo to yield a clear, colorless oil (220 mg; 88% yield). ^{1}H NMR (C_7D_8): δ 7.76 and 7.19 (t, 4H, *o*-Ph, $^3J_{H-H}$ = 7.5 Hz, $^3J_{H-P}$ = 7.5 Hz), 7.58 and 7.54 (dd, 4H, *m*-Ph, $^3J_{H-H}$ = 2.5 Hz, $^3J_{H-H}$ = 7.5 Hz), 6.99 (m, 2H, *p*-Ph), 2.33 and 1.01 (dd, 4H, ring CH_2, $^2J_{H-H}$ = 14.5 Hz, $^2J_{H-P}$ = 3.5 Hz), 0.76 (ABX m, 4H, ring CH_2, $^2J_{H-H}$ = 13.5 Hz, $^2J_{H-P}$ = 9.0 Hz), 0.58, 0.33, 0.30 and 0.12 (s, 12H, SiMe_2). ^{31}P{^{1}H} NMR (C_6D_6): δ −38.8 (s, 1P, uncoordinated phosphine), −44.7 (s, 1P, coordinated phosphine, 120 Hz peak width at half-height).

***anti*-GaCl[P$_2$N$_2$] (2).** To a slurry of $GaCl_3$ (77 mg; 0.44 mmol) in toluene (5 mL) was added a toluene solution (10 mL) of *anti*-$Li_2(THF)_2[P_2N_2]$ (300 mg; 0.44 mmol). The reaction mixture was then stirred for 12 h. The reaction mixture was passed through a frit lined with Celite to remove LiCl. The solvent was then removed in vacuo to yield a white solid. The residue was taken up in a minimum amount of toluene (approximately 3 mL). Slow evaporation of the solvent afforded large colorless plates (200 mg; 74% yield). ^{1}H NMR (C_7D_8): δ 7.66 and 7.19 (t, 4H, *o*-Ph, $^3J_{H-H}$ = 8.5 Hz, $^3J_{H-P}$ = 8.5 Hz), 7.58 and 7.56 (dd, 4H, *m*-Ph, $^3J_{H-H}$ = 7.0 Hz, $^3J_{H-H}$ = 8.5 Hz), 7.00 (m, 2H, *p*-Ph), 2.37 and 1.02 (dd, 4H, ring CH_2, $^2J_{H-H}$ = 14.5 Hz, $^2J_{H-P}$ = 3.5 Hz), 0.68 (ABX m, 4H, ring CH_2, $^2J_{H-H}$ = 16.5 Hz, $^2J_{H-P}$ = 9.5 Hz), 0.58, 0.36, 0.28 and 0.12 (s, 12H, SiMe_2). ^{31}P{^{1}H} NMR (C_6D_6): δ −36.6 (s, 1P, coordinated phosphine, 20 Hz peak width at half-height), −38.0 (s, 1P, uncoordinated phosphine). MS: *m*/*e* 638 (M^+). Anal. Calcd for $C_{24}H_{42}ClGaN_2P_2Si_4$: C, 45.18; H, 6.63; N, 4.39. Found: C, 45.42; H, 6.59; N, 4.30.

***syn*-AlCl[P$_2$N$_2$] (3). Method 1.** To a slurry of $AlCl_3$ (110 mg; 0.82 mmol) in toluene (10 mL) was added a toluene solution (10 mL) of *syn*-Li_2(dioxane)$[P_2N_2]$ (500 mg; 0.79 mmol). The reaction mixture was stirred for 12 h and then passed through a frit lined with Celite to remove LiCl. The solvent was removed in vacuo to yield a white solid. The residue was taken up in a minimum amount of toluene (approximately 4 mL). Slow evaporation of the solvent yielded large colorless plates (470 mg; 100% yield).

Method 2. 1 (200 mg; 0.34 mmol) was dissolved in 10 mL toluene and placed in a reactor bomb. The headspace was evacuated, and the contents of the bomb heated to 100 °C for 3 days with stirring. The solvent was then removed in vacuo to yield a white solid, which was taken up in a minimum amount of toluene (approximately 2 mL). Slow evaporation of the solvent quantitatively afforded colorless plates. ^{1}H NMR (C_6D_6): δ 7.95 (t, 4H, *o*-Ph, $^3J_{H-H}$ = 8.5 Hz, $^3J_{H-P}$ = 8.5 Hz), 7.10 (m, 6H, *m*,*p*-Ph), 0.97 (ABX m, 8H, ring CH_2, $^2J_{H-H}$ = 15.0 Hz, $^2J_{H-P}$ = 9.5 Hz), 0.29 and 0.22 (s, 12H, SiMe_2). ^{31}P{^{1}H} NMR (C_6D_6): δ −43.6 (s, 340 Hz peak width at half-height). MS: *m*/*e* 595 (M^+). Anal. Calcd for $C_{24}H_{42}AlClN_2P_2Si_4$: C, 48.42; H, 7.11; N, 4.71. Found: C, 48.68; H, 7.12; N, 4.55.

***syn*-GaCl[P$_2$N$_2$] (4). Method 1.** To a slurry of $GaCl_3$ (230 mg; 1.3 mmol) in toluene (10 mL) was added a toluene solution (10 mL) of *syn*-Li_2(dioxane)$[P_2N_2]$, (750 mg; 1.2 mmol). The reaction mixture was stirred for 12 h. The reaction mixture was then passed through a frit lined with Celite to remove LiCl. The solvent was removed in vacuo to yield a white solid. The residue was taken up in a minimum amount of toluene (approximately 5 mL). Slow evaporation of the solvent yielded large colorless plates (660 mg; 88% yield).

Method 2. 2 (200 mg; 0.31 mmol) was dissolved in 10 mL toluene and placed in a reactor bomb. The headspace was evacuated and the contents of the bomb heated to 100 °C for 3 days with stirring. The solvent was removed in vacuo and the resultant colorless oil taken up in a minimum of toluene. Slow evaporation of the solvent resulted in colorless plates of **4** (180 mg, 92% yield). ^{1}H NMR (C_6D_6): δ 7.90 (t, 4H, *o*-Ph, $^3J_{H-H}$ = 7.9 Hz, $^3J_{H-P}$ = 7.9 Hz), 7.09 (m, 6H, *m*,*p*-Ph), 0.96 (ABX m, 8H, ring CH_2, $^2J_{H-H}$ = 13.0 Hz, $^2J_{H-P}$ = 14.0 Hz), 0.28 and 0.19 (s, 12H, SiMe_2). ^{31}P{^{1}H} NMR (C_6D_6): δ −41.5 (s, 65 Hz peak width at half-height).

Kinetics of the Inversion Reactions. The first-order conversion of the *anti*-MCl$[P_2N_2]$ complexes to the *syn*-MCl$[P_2N_2]$ complexes (M = Al, Ga) was monitored by ^{1}H NMR spectroscopy by following the disappearance of the anti complex and the appearance of the syn complex over time. ~0.1 M C_7D_8 solutions of the pure anti complexes were placed in sealed NMR tubes and immersed in oil baths (maintained at a specific temperature) for a known length of time. The tubes were then removed from the oil baths and the spectra taken at room temperature. The irreversibility of the conversion did not necessitate quenching the reaction by freezing the samples. A similar protocol was followed in examining the behavior of the protonated derivatives *anti*-$H_2[P_2N_2]$ and *syn*-$H_2[P_2N_2]$; in this case the conversion was followed by ^{31}P{^{1}H} NMR spectroscopy in both C_7D_8 and a 4:1 mixture of C_6D_5Br/C_6D_6.

X-ray Crystallographic Analyses of *anti*-GaCl[P$_2$N$_2$] (2) and *syn*-GaCl[P$_2$N$_2$] (4). Crystallographic data appear in Table 1. The final unit-cell parameters were obtained by least-squares on the setting angles for 25 reflections with 2θ = 45.7−68.2° for **2**; and 24 016 reflections with 2θ = 5.0−63.1° for **4**. The intensities of three standard reflections, measured every 200 reflections throughout the data collections, decayed linearly for **2** (4.6%). The data were processed[15] and corrected for Lorentz and polarization effects, decay (for **2**), and absorption (empirical, based on azimuthal scans for **2**, and symmetry analysis of symmetry-equivalent data for **4**).

Table 1. Crystallographic Data

	anti-GaCl$[P_2N_2]$ (**2**)	*syn*-GaCl$[P_2N_2]$ (**4**)
empirical formula	$C_{34}H_{42}ClGaN_2P_2Si_4$	$C_{34}H_{42}ClGaN_2P_2Si_4$
fw	638.07	638.07
cryst syst	orthorhombic	orthorhombic
space group	*Pbca* (No. 61)	$P2_12_12_1$ (No. 19)
a, Å	17.237(2)	8.9331(8)
b, Å	24.650(2)	17.5651(6)
c, Å	15.887(2)	21.2421(7)
V, Å^3	6750(1)	3333.1(3)
Z	8	4
ρ_{calc}, g/cm^3	1.256	1.271
T, °C	21	−93
radiation	Cu	Mo
λ, Å	1.541 78	0.710 69
μ, cm^{-1}	42.20	11.61
transmission factors	0.56−1.00	0.79−1.01
R	0.036[a]	0.075[b]
R_w	0.032[a]	0.075[b]

[a] $R(F) = \sum||F_o| - |F_c||/\sum|F_o|$, $R_w(F) = (\sum w(|F_o| - |F_c|)^2/\sum w|F_o|^2)^{1/2}$. [b] $R(F^2) = \sum|F_o^2 - F_c^2|/\sum|F_o^2|$, $R_w(F^2) = (\sum w(|F_o^2| - |F_c^2|)^2/\sum w|F_o|^4)^{1/2}$.

(13) Fryzuk, M. D.; Love, J. B.; Rettig, S. J. *J. Chem. Soc., Chem. Commun.* **1996**, *24*, 2783.
(14) Fryzuk, M. D.; Love, J. B. Unpublished results.

Table 2. Selected Bond Lengths (Å) for *anti*-GaCl[P_2N_2] (**2**) (Left) and *syn*-GaCl[P_2N_2] (**4**) (Right)

Cl(1)−Ga(1)	2.189(1)	Cl(1)−Ga(1)	2.2525(9)
N(1)−Ga(1)	1.899(3)	N(1)−Ga(1)	1.968(2)
N(2)−Ga(1)	1.887(3)	N(2)−Ga(1)	1.966(2)
P(1)−Ga(1)	2.360(1)	P(1)−Ga(1)	2.4930(8)
		P(2)−Ga(1)	2.4695(8)

Table 3. Selected Bond Angles (deg) for *anti*-GaCl[P_2N_2] (**2**) (Left) and *syn*-GaCl[P_2N_2] (**4**) (Right)

		P(1)−Ga(1)−P(2)	164.63(3)
N(1)−Ga(1)−N(2)	116.7(1)	N(1)−Ga(1)−N(2)	119.4(1)
Cl(1)−Ga(1)−P(1)	112.49(5)	Cl(1)−Ga(1)−P(1)	98.04(3)
		Cl(1)−Ga(1)−P(2)	97.32(3)
Cl(1)−Ga(1)−N(1)	114.3(1)	Cl(1)−Ga(1)−N(1)	122.06(8)
Cl(1)−Ga(1)−N(2)	116.0(1)	Cl(1)−Ga(1)−N(2)	118.54(8)
Ga(1)−P(1)−C(13)	125.9(2)	Ga(1)−P(1)−C(13)	130.3(1)
		Ga(1)−P(2)−C(19)	127.9(1)
P(1)−Ga(1)−N(1)	97.5(1)		
P(1)−Ga(1)−N(2)	96.5(1)		

The structures were solved by the Patterson method. The nonhydrogen atoms were refined with anisotropic thermal parameters. Hydrogen atoms were fixed in calculated positions with C−H = 0.98 Å and $B_H = 1.2B_{\text{bonded atom}}$. A secondary extinction correction was applied for **2** (Zachariasen type, isotropic), the final value of the extinction coefficients being $1.16(2) \times 10^{-6}$. No extinction correction was necessary for **4**. Neutral atom scattering factors and anomalous dispersion corrections were taken from the *International Tables for X-ray Crystallography*.[16] Parallel refinements of the opposite enantiomer of **4** (for the particular crystals used) gave significantly higher residuals, the *R* and R_w factor ratios being 1.42 and 1.56, respectively.

Selected bond lengths and bond angles appear in Tables 2 and 3. Tables of full crystallographic data, final atomic coordinates and equivalent isotropic thermal parameters, anisotropic thermal parameters, all bond lengths and angles, torsion angles, intermolecular contacts, and least-squares planes are included as Supporting Information.

Results and Discussion

Synthesis of *anti*-[P_2N_2] Complexes of Aluminum and Gallium. The reaction of the dilithio salt *anti*-$Li_2(THF)_2[P_2N_2]$[13] with $AlCl_3$ or $GaCl_3$ in toluene at 25 °C for 12 h generates good yields of the monomeric chlorides *anti*-AlCl[P_2N_2] (**1**) and *anti*-GaCl[P_2N_2] (**2**) (eq 1). The ^{1}H NMR spectra of both products are similar and show four singlets arising from the silyl methyl protons (SiCH_3) and two distinct ortho phenyl resonances. The ^{31}P{^{1}H} NMR spectrum of **1** consists of two singlets; a sharp peak at −38.8 ppm characteristic of an uncoordinated phosphorus-31 nucleus within the [P_2N_2] macrocycle, and a broad resonance upfield at −44.7 ppm, due to the coordinated phosphine ($\Delta_{1/2}$ = 120 Hz). The broadness of this latter peak is the result of coordination to the quadrupolar ^{27}Al nucleus (^{27}Al, $I = {}^5/_2$, 100% natural abundance).[17,18] The gallium analogue **2** also exhibits two peaks in the ^{31}P{^{1}H} NMR spectrum; however, the chemical shifts of the peaks arising from coordinated and uncoordinated phosphine donors are reversed, with the resonance due to the coordinated phosphine downfield of the free phosphine (−36.6 and −38.0 ppm, respectively). As in **1**, the peak arising from the coordinated phosphine in **2** is broadened by interaction with a quadrupolar nucleus (^{69}Ga, $I = {}^3/_2$, 60.4% abundance; ^{71}Ga, $I = {}^3/_2$, 39.4% abundance)[17,18] although to a lesser extent ($\Delta_{1/2}$ = 20 Hz) than in the aluminum analogue **1**.

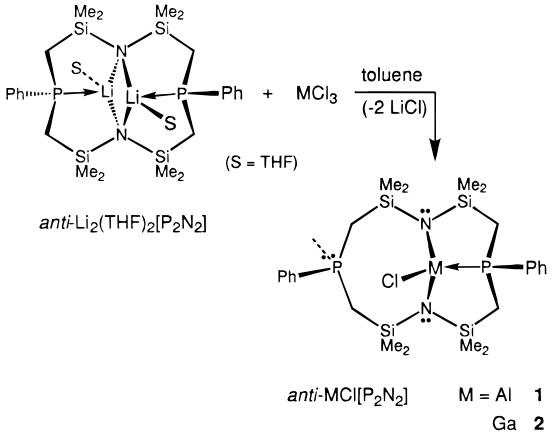

(1)

While the gallium species **2** was isolated as a crystalline solid, the aluminum derivative **1** resisted crystallization and could only be obtained as an air- and moisture-sensitive oil which prevented elemental analyses. Although we were unable to isolate **1** in the solid state, the similarity of the ^{1}H and ^{31}P{^{1}H} NMR spectra of **1** and **2** indicate that the general structural features present in the structural analysis of **2** also hold true for **1**.

Synthesis of *syn*-[P_2N_2] Complexes of Aluminum and Gallium. Good yields of the monomeric chlorides *syn*-AlCl[P_2N_2] (**3**) and *syn*-GaCl[P_2N_2] (**4**) were effected via the reaction of the ancillary ligand *syn*-Li_2(dioxane)[P_2N_2][13] with slurries of $AlCl_3$ and $GaCl_3$ in toluene at 25 °C for 12 h (eq 2). The ^{1}H NMR spectra of the products are indicative of C_{2v} symmetric complexes: the four silyl methyl proton resonances (SiCH_3) found for the anti derivatives **1** and **2** are replaced by two peaks of equal intensity in **3** and **4**, while only a single ortho proton signal is now present. The ^{31}P{^{1}H} NMR spectra of **3** and **4** consist of a single peak at −42 ppm, whose broadness is mirrored by the quadrupole moment of the metal, i.e., Al ($\Delta_{1/2}$ = 340 Hz) > Ga ($\Delta_{1/2}$ = 65 Hz).

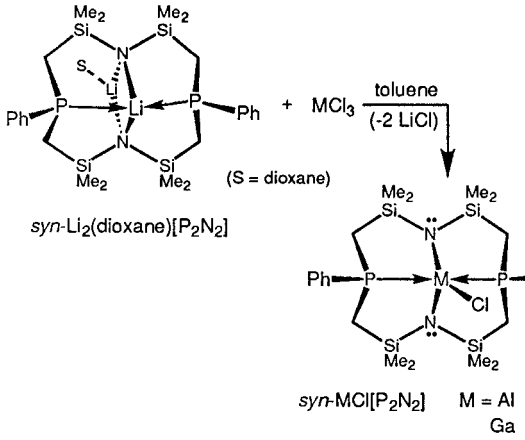

(2)

Compounds **3** and **4** are colorless, thermally stable, air- and moisture-sensitive, crystalline solids. The ^{1}H and ^{31}P{^{1}H} NMR spectra indicate that **3** and **4** have symmetric solution structures. Solid-state structural studies of *anti*-GaCl[P_2N_2] (**2**) and *syn*-GaCl[P_2N_2] (**4**) were undertaken to further delineate the nature of these compounds.

(15) (a) *teXsan*: *Crystal Structure Analysis Package*, Version 1.7; Molecular Structure Corp.: The Woodlands, TX, 1995. (b) *d*TREK*: *Area Detector Software*; Molecular Structure Corp.: The Woodlands, TX, 1997.

(16) (a) *International Tables for X-ray Crystallography*; Kynoch Press: Birmingham, U.K. (present distributor Kluwer Academic Publishers: Boston, MA), 1974; Vol. IV, pp 99−102. (b) *International Tables for Crystallography*; Kluwer Academic Publishers: Boston, MA, 1992; Vol. C, p 200−206.

(17) Delpuech, J. J. *NMR of Newly Accessible Nuclei*; Academic Press: New York, 1983; Vol. 2.

(18) Akitt, J. W. *Prog. NMR Spectrosc.* **1989**, *21*, 1.

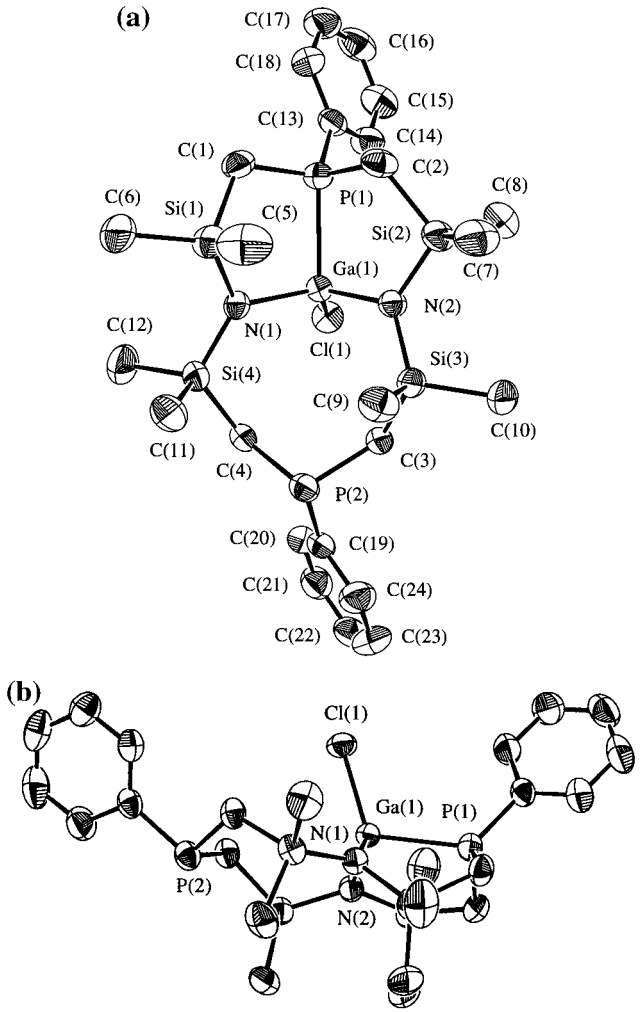

Figure 1. (a) Molecular structure of *anti*-GaCl[P_2N_2] (**2**); 33% probability thermal ellipsoids are shown. Hydrogen atoms are omitted for clarity. (b) Side view of *anti*-GaCl[P_2N_2] (**2**).

Structure of *anti*-GaCl[P_2N_2] (2) and *syn*-GaCl[P_2N_2] (4). Evaporation of a saturated toluene solution of **2** resulted in large colorless plates that were suitable for single-crystal X-ray diffraction. The molecular structure and numbering scheme are illustrated in Figure 1; complete details of the structural analyses of **2** and **4** are presented in Table 1. In **2** the [P_2N_2] ligand retains an *anti*-configuration, with coordination of a single phosphorus to the central metal observed. In this configuration, the gallium atom adopts a distorted tetrahedral geometry, which is common for the lighter members of group 13.[19] The macrocyclic ligand does impose some distortion as can be seen from the N(1)−Ga(1)−N(2) angle of 116.7(1)°. The other angles anchored by Ga range from 116.0(1)° to 96.5(1)°. P(1) must distort slightly in order to coordinate to gallium, as is illustrated by the Ga(1)−P(1)−C(13) angle of 125.9(2)°. Otherwise, P(1) and P(2) exhibit typical bond angles, falling within normal ranges associated with tetrahedral geometries. The Ga−Cl bond length of 2.189(1) Å is only slightly shorter than those reported for a number of similar macrocyclic systems (i.e., Ga(tetraphenylporphyrinato)-Cl = 2.196(2) Å,[20] Ga(phthalocyaninato)Cl = 2.217(1) Å,[21] Ga(dibenzotetramethyltetraaza[14]annulene)Cl = 2.222(2) Å[22]), but still longer than for Cp*Ga systems.[23]

The Ga(1)−P(1) distance of 2.360(1) Å is comparable to the shortest reported gallium−phosphorus distance of 2.353(2) Å found in $GaCl_3 \cdot PMe_3$.[24] This distance, indicative of the Lewis acidic nature of the metal center, is approximately the sum of the covalent radii (approximately 2.30 Å).[25] Most neutral phosphine adducts of gallium exhibit Ga−P bond distances in the range of 2.4−2.7 Å.[26−29] The Ga−N distances of 1.899(3) and 1.887(3) Å are normal in terms of gallium−amide bond lengths and are somewhat shorter than those reported for the above-mentioned macrocyclic systems, where some degree of delocalization is present.[20,21] The most valid comparison is with the compounds $Ga[N(SiMe_3)_2]_3$ (1.870(6) Å)[20,21,30,31] and $GaCl[N(SiMe_3)_2]_2$ (1.8344(4) and 1.844(4) Å)[31] in which the Ga−N distances were determined to fall well within the established range of 1.85−1.92 Å for gallium−amide bonds.[30] A list of selected bond lengths and angles for **2** and **4** can be found in Tables 2 and 3.

Evaporation of a saturated toluene solution of **4** resulted in large colorless plates that were suitable for single-crystal X-ray diffraction. The molecular structure and numbering scheme are illustrated in Figure 2. The structural analysis confirms that **4** is monomeric and that the macrocycle has the *syn* configuration; furthermore, the distorted trigonal bipyramidal geometry of the gallium center is clearly evident. Although the preferred geometry for five-coordinate gallium is trigonal bipyramidal, macrocyclic nitrogen ligand systems such as phthalocyanine (Pc)[21] and octaethylporphyrin (OEP)[32] induce square pyramidal coordination for aluminum. The difference between these systems and the [P_2N_2] system can be attributed to the more rigid nature of the delocalized N_4 ring system in Pc and OEP.

The phosphine donors of **4** occupy the axial positions, defining a P(1)−Ga(1)−P(2) angle of 164.63(3)°. The two amides, the Ga center, and the chloride define a plane (mean deviation = 0.0032 Å) whose members form angles of 122.06(8)°, 119.4(1)°, and 118.54(8)° with each other. The metal perches slightly above the plane defined by the two amides and the two phosphines. Both phosphines experience normal tetrahedral geometries with two notable exceptions: P(1) maintains a Ga(1)−P(1)−C(13) angle of 130.3(1)°, ∼20° more than that expected for four-coordinate phosphorus. A similar distortion is evident for P(2) (Ga(1)−P(2)−C(19) = 127.9(1)°). This bending back of the phenyl rings on the phosphorus donors is an indication of the slight distortion required for the [P_2N_2] ligand system to accommodate the small gallium nucleus.

(19) Mole, T.; Jeffrey, E. A. *Organoaluminum Compounds*; Elsevier: Amsterdam, 1972.
(20) Coutsolelos, A.; Guilard, R.; Bayeul, D.; Lecomte, C. *Polyhedron* **1986**, *5*, 1157.
(21) Wynne, K. J. *Inorg. Chem.* **1984**, *23*, 4658.
(22) Atwood, D. A.; Atwood, V. O.; Cowley, A. H.; Atwood, J. L.; Roman, E. *Inorg. Chem.* **1992**, *31*, 3871.
(23) Beachley, O. T.; Hallock, R. B.; Zhang, H. M.; Atwood, J. L. *Organometallics* **1985**, *4*, 1675.
(24) Carter, J. C.; Jugie, G.; Enjalbert, R.; Galy, J. *Inorg. Chem.* **1978**, *17*, 1248.
(25) Boardman, A.; Small, R. W. H.; Worrall, I. J. *Inorg. Chim. Acta* **1986**, *119*, L13.
(26) Bradley, D. C.; Chudzynska, H.; Faktor, M. M.; Frigo, D. M.; Hursthouse, M. B.; Hussain, B.; Smith, L. M. *Polyhedron* **1988**, *14*, 1289.
(27) Banks, M. A.; Beachley, O. T., Jr.; Maloney, J. D.; Rogers, R. D. *Polyhedron* **1990**, *9*, 335.
(28) O'Hare, D.; Foord, J. S.; Page, T. C. M.; Whitaker, T. J. *J. Chem. Soc., Chem. Commun.* **1991**, 1445.
(29) Wells, R. L.; Aubuchon, S. R.; Self, M. F.; Jasinski, J. P.; Woudenberg, R. C.; Butcher, R. J. *Organometallics* **1992**, *11*, 3370.
(30) Atwood, D. A.; Atwood, V. O.; Cowley, A. H.; Jones, R. A.; Atwood, J. L.; Bott, S. G. *Inorg. Chem.* **1994**, *33*, 3251.
(31) Brothers, P. J.; Wehmschulte, R. J.; Olmstead, M. M.; Ruhlandt-Senge, K.; Parkin, S. R.; Power, P. P. *Organometallics* **1994**, *13*, 2792.
(32) Dolphin, D. *The Porphyrins*; Academic Press: New York, 1978; Vol. 1.

The gallium−chloride distance of 2.2525(9) Å compares well with that found in Ga(Pc)Cl (2.179(6) Å).[21] The gallium−phosphorus bond lengths of 2.4930(8) Å and 2.4695(8) Å are well within the normal range associated with such bonds (∼2.4−2.7 Å).[26−29] The gallium−nitrogen distances of 1.968(2) and 1.966(2) Å are normal in terms of gallium−amide bonds.[31]

Conversion of *anti*-MCl[P_2N_2] Complexes to *syn*-MCl[P_2N_2] Complexes (M = Al, Ga). Previous work from our group established that the addition of *anti*-$Li_2(THF)_2[P_2N_2]$ to $ScCl_3(THF)_3$ at room-temperature resulted in the formation of $\{syn\text{-}[P_2N_2]Sc\}_2(\mu\text{-}Cl)_2$.[14] That the syn compound was produced instead of the anti analogue was surprising, and indicated that pyramidal inversion and subsequent coordination of the free phosphine had occurred. However, the high rate of inversion did not allow study of the kinetics of this system. The isolation of the four-coordinate anti compounds **1** and **2**, and the observation that these species could be converted to the five-coordinate syn compounds **3** and **4** provided for a potentially better system for examining the activation parameters of this particular type of pyramidal inversion (eq 3). Rate plots, kinetic data for the two systems, along with Arrhenius plots are present as Supporting Information. Selected transition state parameters are listed in Table 4.

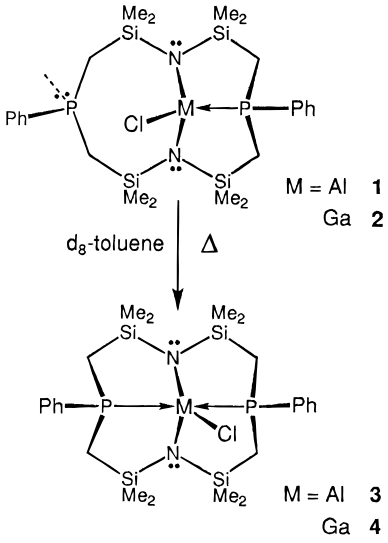

(3)

Plots of ln{1/% *anti*-MCl[P_2N_2]} vs time yielded straight lines at all temperatures measured for both the aluminum and the gallium systems. The first-order nature of the inversion was further confirmed by a concentration study of the aluminum system in which various concentrations of **1** (∼0.05−0.005 M) were heated at 80 and 100 °C for 8 h. The invariance of the rate of inversion with concentration points to a simple intramolecular process being operative.[9] To further illustrate that the process being studied is a simple pyramidal inversion, a variable temperature $^{31}P\{^1H\}$ NMR study was performed on *anti*-AlCl[P_2N_2] (**1**) and *anti*-GaCl[P_2N_2] (**2**). The $^{31}P\{^1H\}$ NMR spectra of **1** and **2** at 90 °C were identical to the room-temperature spectra of these species, and thus the solid-state structure of **2** was concluded to be representative of the room-temperature solution structures of both **1** and **2**.

The transition state parameters for the two systems are quite similar: the Gibb's free energy of activation (at 100 °C) was found to be 29.1 kcal mol^{-1} for the aluminum system, and 30.1 kcal mol^{-1} for the gallium system. This represents a lowering of the barrier to pyramidal inversion of about 5 kcal mol^{-1};

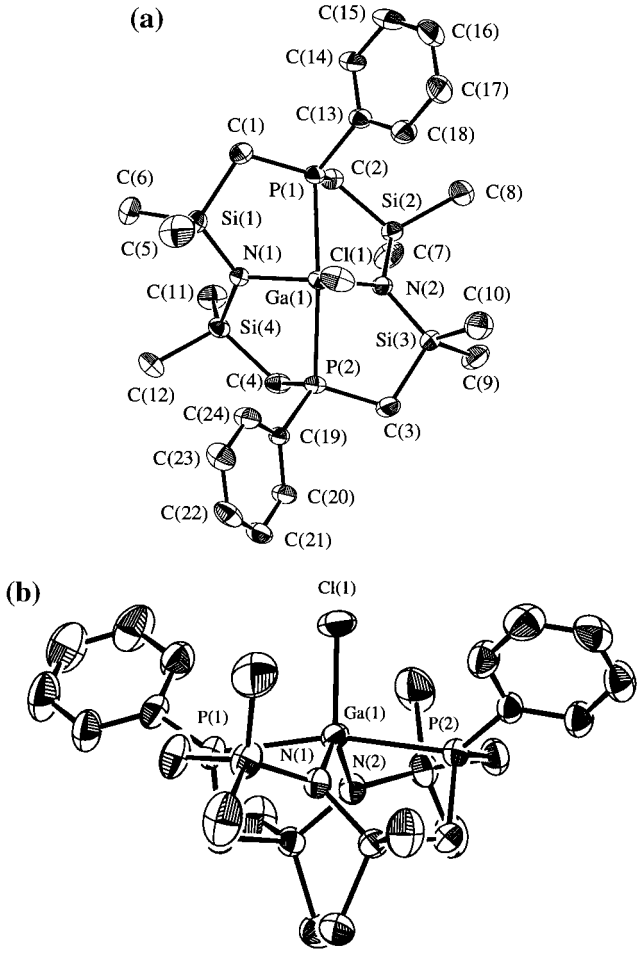

Figure 2. (a) Molecular structure of *syn*-GaCl[P_2N_2] (**4**); 50% probability thermal ellipsoids are shown. Hydrogen atoms are omitted for clarity. (b) Side view of *syn*-GaCl[P_2N_2] (**4**).

Table 4. Transition State Parameters for the Conversion of *anti*-MCl[P_2N_2] to *syn*-MCl[P_2N_2] (M = Al, Ga) in C_7D_8

function	M = Al	M = Ga
$\Delta H^{\ddagger}$, kcal mol^{-1}	20.0 ± 1.4	17.5 ± 1.2
$\Delta S^{\ddagger}$, cal K^{-1} mol^{-1}	−24.4 ± 3.0	−33.8 ± 2.5
$\Delta G_{373}^{\ddagger}$, kcal mol^{-1}	29.1 ± 2.7	30.1 ± 2.7
correlation, *R*	0.985	0.985

activation energies for trialkylphosphines are typically in the range 35−38 kcal mol^{-1}.[1,6−9] Previous studies have established that such inversions occur via a planar transition state where the phosphine is sp^2-hybridized. Consequently, the p-orbital can engage in overlap with orbitals on adjacent atoms to stabilize the transition state and lower the barrier to inversion. Most often this interaction has been viewed as a π-overlap as in arylphosphines ($p_\pi-p_\pi$),[8,9,33] diphosphines,[8,9,33−36] or silylphosphines ($p_\pi-d_\pi$).[8,37] For arylphosphines, a lowering of the barrier of approximately 2−3 kcal mol^{-1} per aryl substituent[1] has been estimated. Incorporation of the phosphorus center into a phosphole ring results in 6π-electron systems in which electron delocalization is at a maximum in the planar transition state

(33) Rakshys, J. W.; Taft, R. W.; Sheppard, W. A. *J. Am. Chem. Soc.* **1968**, *90*, 5236.
(34) Lambert, J. B.; Mueller, D. C. *J. Am. Chem. Soc.* **1966**, *88*, 3669.
(35) Lambert, J. B.; Jackson, G. F.; Mueller, D. C. *J. Am. Chem. Soc.* **1968**, *90*, 6401.
(36) Lambert, J. B.; Jackson, G. F.; Mueller, D. C. *J. Am. Chem. Soc.* **1970**, *92*, 3093.
(37) Baechler, R. D.; Mislow, K. *J. Am. Chem. Soc.* **1970**, *92*, 4758.

Table 5. Transition State Parameters for the Conversion of *anti*/*syn*-$H_2[P_2N_2]$ to *syn*/*anti*-$H_2[P_2N_2]$ in C_7D_8

function	*anti*- to *syn*-	*syn*- to *anti*-
$\Delta H^{\ddagger}$, kcalmol^{-1}	18.9 ± 2.3	21.0 ± 2.2
$\Delta S^{\ddagger}$, cal K^{-1} mol^{-1}	-36.0 ± 4.2	-30.0 ± 3.1
$\Delta G_{373}^{\ddagger}$, kcal mol^{-1}	32.3 ± 2.5	32.2 ± 2.5
correlation, R	0.993	0.983

relative to the pyramidal ground state.[38−40] This results in barriers to inversion most often in the range of 15−18 kcal mol^{-1}. However, to our knowledge, the effect of an electropositive metal center in proximity to a phosphorus inversion process has never been cited. To more accurately assess the role of the metal, it was necessary to obtain the transition state parameters for the inversion of phosphorus in the metal-free, protonated analogues *syn*- and *anti*-$H_2[P_2N_2]$.

Pyramidal Inversion of Phosphorus in *anti*-$H_2[P_2N_2]$ and *syn*-$H_2[P_2N_2]$. *anti*-$H_2[P_2N_2]$ and *syn*-$H_2[P_2N_2]$ undergo pyramidal inversion at phosphorus in a different manner than the metal complexes *anti*-$MCl[P_2N_2]$ (M = Al (**1**), Ga (**2**)). Whereas the aluminum and gallium complexes undergo irreversible first-order reactions, the protonated derivatives are in equilibrium (eq 4).

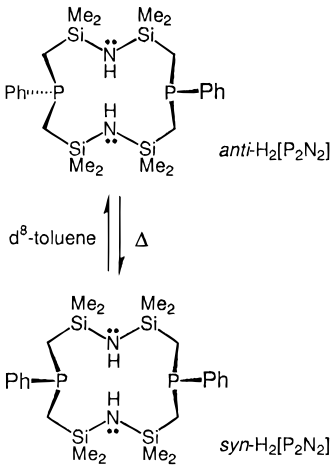

(4)

To ensure that the protonated derivatives were in equilibrium, the kinetics were studied in both directions, starting with *anti*-$H_2[P_2N_2]$ and also with *syn*-$H_2[P_2N_2]$. All kinetic runs were performed until the contents of the tubes had equilibrated to a ~50/50 mixture of the syn and anti isomers. It is worth noting that the protonated derivatives invert approximately 20 and 70 times *slower* than the gallium and aluminum complexes, respectively. Rate plots, the kinetics of the two systems, and the Arrhenius plots can be found in the Supporting Information. Transition state parameters of the two systems are presented below (Table 5).

As expected for an equilibrium, the transition state parameters are the same (within experimental error) regardless of the direction studied. The $\Delta G_{373}^{\ddagger}$ values for the two systems are 32.3 (anti to syn) and 32.2 (syn to anti) kcal mol^{-1}. These numbers are in agreement with those found in the literature; monoaryldialkylphosphines usually have barriers of about 32 kcal mol^{-1}.[1] What is unusual is the large negative value of $\Delta S^{\ddagger}$ (−36.0, −30.0 cal K^{-1} mol^{-1}). Since the planar transition state is more ordered than the pyramidal ground state, a small negative entropy of activation for acyclic phosphines would be expected (approximately −3 cal K^{-1} mol^{-1}).[7] Two factors may contribute to the large negative entropy of activation observed here: (i) ring strain and (ii) solvation effects. The first factor, ring strain, can be discounted since phosphetanes, in which the phosphorus atom is part of a four-membered ring, exhibit normal barriers to pyramidal inversion and $\Delta S^{\ddagger}$ values of −8 cal K^{-1} mol^{-1}.[41] With regard to the second possible factor, if the ground state and the transition state interact with solvent molecules to different degrees, this could result in anomalously large entropy effects. This has been found previously for nitrogen-based systems. For example, the value of $\Delta S^{\ddagger}$ for 1,2,2-trimethylaziridine in a halogenated solvent such as chloroform (38 cal K^{-1} mol^{-1}) is much larger than in benzene or acetone (15 cal K^{-1} mol^{-1}).[42] This is due to a greater degree of hydrogen bonding in the ground state than in the transition state for chloroform vs benzene or acetone. To examine the possible role that solvent may play in these systems, we repeated the study of the conversion of *syn*-$H_2[P_2N_2]$ to *anti*-$H_2[P_2N_2]$ in 4:1 C_6D_6/C_6D_5Br. The rate and Arrhenius plots for this system are available as Supporting Information. The transition state data for the pyramidal inversion of phosphorus in 4:1 C_6D_6/C_6D_5Br are similar to those determined in C_7D_8: $\Delta G_{373}^{\ddagger} = 31.4 \pm 3.7$ kcal mol^{-1}, $\Delta H^{\ddagger} = 11.7 \pm 1.8$ kcal mol^{-1}, and $\Delta S^{\ddagger} = -53.0 \pm 4.8$ cal K^{-1} mol^{-1}. The large negative value of $\Delta S^{\ddagger}$ implies that C_6D_5Br interacts with the transition state to a greater degree than the ground state. As well, $\Delta S^{\ddagger}$ has a larger negative value than for the inversion in C_7D_8. The entropy of activation in C_7D_8 (−36.0, −30.0 cal K^{-1} mol^{-1}) points toward the transition state being stabilized by π-stacking or some other sort of interaction with the solvent. However, in the absence of further study, this still remains speculative.

Mechanism of Pyramidal Inversion of Phosphorus in $MCl[P_2N_2]$ (M = Al, Ga). The results obtained for the metal complexes may now be compared with the metal-free protonated analogues. As already mentioned, the aluminum and gallium compounds invert at rates that are approximately 70 and 20 times faster, respectively, than the metal-free macrocyclic diamines. Because of the logarithmic relationship between the rate constant and the free energy of activation, this corresponds to $\Delta G_{373}^{\ddagger}$ values which are 3.2 and 2.2 kcal mol^{-1} lower than that of the protonated derivatives, respectively. However, given the uncertainty present in the data (±2.5 kcal mol^{-1} in the diamines, ±2.7 kcal mol^{-1} in the metal complexes), the difference in the activation barriers becomes moot. Nevertheless, the rates are reproducibly different and can be discussed. A possible mechanism of phosphorus inversion for the *anti*-$MCl[P_2N_2]$ derivatives is outlined in Scheme 1.

In Scheme 1, the metal center directly assists in the inversion of the phosphorus. As implied in the crystal structure of **2**, the lone pair on the sp^3-hybridized phosphorus atom is oriented away from the metal center. The electrophilic metal atom attracts the minor lobe toward it, resulting in a planar sp^2-hybridized phosphorus atom. Note that this interaction is not a π-overlap, but a σ-overlap between a phosphorus-based p-orbital and a p-type orbital on the metal. The attraction of the metal for the lone pair results in the simultaneous formation of a dative bond and inversion of the phosphorus. The mechanism proposed is much like that of a typical S_N2 reaction in which the carbon atom is attacked from the more hindered side, passing through

(38) Laporte, F.; Mercier, F.; Ricard, L.; Mathey, F. *J. Am. Chem. Soc.* **1994**, *116*, 3306.
(39) Egan, W.; Tang, R.; Zon, G.; Mislow, K. *J. Am. Chem. Soc.* **1970**, *92*, 1442.
(40) Egan, W.; Tang, R.; Zon, G.; Mislow, K. *J. Am. Chem. Soc.* **1971**, *93*, 6205.
(41) Cremer, S. E.; Chorvat, R. J.; Davis, D. W. *Tetrahedron Lett.* **1968**, *55*, 5799.
(42) Jautelat, M.; Roberts, J. D. *J. Am. Chem. Soc.* **1969**, *91*, 642.

Scheme 1

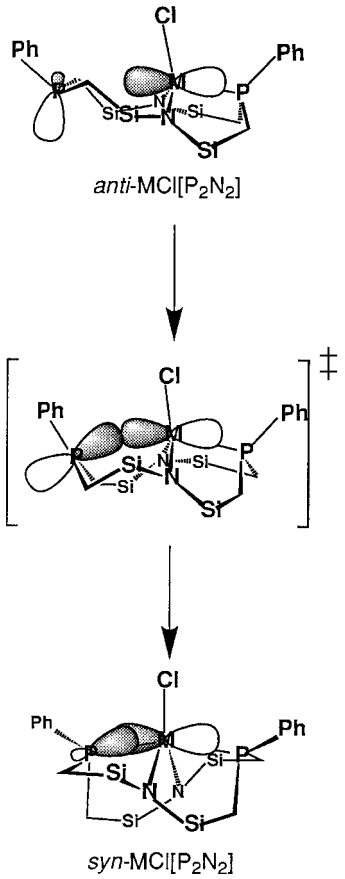

a planar sp^2-hybridized carbocation transition state on its way to the final product whose chirality is opposite that of the original reactant.[43]

It may be argued that the similarity in the values of $\Delta G_{373}^{\ddagger}$ for the two systems suggests a simple inversion at phosphorus, followed by coordination to the metal. However, if the inversion occurred without the influence of the metal, the substitution of gallium for aluminum would have no effect on $\Delta S^{\ddagger}$, since the transition state does not involve bond formation. The difference in $\Delta S^{\ddagger}$ for Al (-24.4 cal K^{-1} mol^{-1}) vs Ga (-33.8 cal K^{-1} mol^{-1}) is consistent with a transition state involving the formation of a phosphorus-metal bond.

Another curious aspect of these systems is the faster rate of inversion for the aluminum compound even though the Gibb's free energy of activation is similar to the gallium analogue. This we attribute to a difference in the entropy of activation. The $\Delta S^{\ddagger}$ values for the aluminum and gallium systems indicate that both systems are entropically disfavored (-24.4 and -33.8 cal K^{-1} mol^{-1}, respectively). However, $\Delta S^{\ddagger}$ for the formation of the gallium compound is approximately 10 cal K^{-1} mol^{-1} more negative than that of the corresponding aluminum complex. This means that the gallium system must attain a more ordered transition state presumably by undergoing a greater conformational rearrangement, i.e., a planar phosphorus engaging in σ-overlap with the gallium atom. The longer gallium−amide bonds as compared to aluminum−amide bonds[44] necessitate the tetrahedral gallium perching higher above the $[P_2N_2]$ cavity than aluminum, resulting in less effective overlap.

(43) Fessenden, R. J.; Fessenden, J. S. *Organic Chemistry*, 4th ed.; Brooks/Cole Publishing Co.: Pacific Grove, 1990.

Summary

By utilizing the macrocyclic ligand system $[P_2N_2]$, we were able to isolate and characterize both anti and syn isomers of the chlorides of aluminum and gallium. It can be argued that the proximity of the metals to an uncoordinated phosphine in complexes of the type *anti*-MCl$[P_2N_2]$ (M = Al (**1**), Ga (**2**)) assists in the inversion and subsequent coordination of this phosphine to yield the *syn*- isomers *syn*-MCl$[P_2N_2]$ (M = Al (**3**), Ga (**4**)). The barrier to pyramidal inversion ($\Delta G_{373}^{\ddagger}$) at phosphorus in these systems was found to be similar to those determined for the metal-free compounds *anti*- and *syn*-$H_2[P_2N_2]$. Therefore, the presence of a Lewis acidic metal center results in an acceleration of the rate of inversion of configuration at phosphorus, although the effect on $\Delta G^{\ddagger}$ is minimal.

Acknowledgment. Financial support was generously provided by the NSERC of Canada in the form of grants to M.D.F. and a postgraduate scholarship to G.R.G.

Supporting Information Available: Complete tables of bond lengths and bond angles, final atomic coordinates, hydrogen atom parameters, anisotropic thermal parameters, torsion angles, intermolecular contacts, least-squares planes, kinetic and Arrhenius plots for the conversion of *anti*-MCl$[P_2N_2]$ (M = Al (**1**), Ga (**2**)) to *syn*-MCl$[P_2N_2]$ (M = Al (**3**), Ga (**4**)), *anti*-$H_2[P_2N_2]$ to *syn*-$H_2[P_2N_2]$, and *syn*-$H_2[P_2N_2]$ to *anti*-$H_2[P_2N_2]$ in C_7D_8 and *syn*-$H_2[P_2N_2]$ to *anti*-$H_2[P_2N_2]$ in 4:1 C_6D_5Br/C_6D_6 and tables of kinetic and Arrhenius data (58 pages). Ordering information is given on any masthead page.

IC9805978

(44) Crystal data for *syn*-AlCl$[P_2N_2]$ (**3**): molecular formula = $C_{24}H_{42}AlClN_2P_2Si_4$; MW = 595.33 g/mol; orthorhombic, space group $P2_12_12_1$ (No. 19), a = 17.553(2) Å, b = 21.155 Å, c = 8.924(1) Å; volume = 3313.7(5) $Å^3$, Z = 4; D_{calcd} = 1.193 g/cm^3, $F(000)$ = 1264.00; μ = 36.99 cm^{-1}. Data collection (294 K): Rigaku AFC6S diffractometer, graphite-monochromated Cu Kα radiation (λ = 1.541 78 Å). The structure was solved by direct methods and refined using the *teXsan* crystal structure analysis package. A total of 4000 reflections were measured of which 3072 reflections ($I > 3\sigma(I)$) were used in the refinement. The final R_w was 0.029 with conventional R = 0.029, GOF = 1.73. Selected bond lengths for **3**: Cl(1)−Al(1) = 2.197 Å; P(1)−Al(1) = 2.481(1) Å; P(2)−Al(1) = 2.465(1) Å; N(1)−Al(1) = 1.886(3) Å; N(2)−Al(1) = 1.909(3) Å.